

Research Article

Efficiency Enhancement of P3HT: PCBM Based Organic Photovoltaic Devices via Incorporation of Bio-synthesized Gold Nanoparticles

Nesrin Tore¹, Elif Parlak¹, Serap Gunes², Umit Ozturk H³, Guldem Utkan³, Akin Denizci A³ and Fevzihan Basarir^{*4}¹Chemistry Institute, TUBITAK Marmara Research Center (MRC), Turkey²Department of Physics, Yildiz Technical University, Turkey³Genetic Engineering and Biotechnology Institute, TUBITAK Marmara Research Center (MRC), Turkey⁴Material Institute, TUBITAK Marmara Research Center (MRC), Turkey***Corresponding author:** Fevzihan Basarir, TUBITAK Marmara Research Center (MRC), Materials Institute, 41470 Gebze, Kocaeli, Turkey, Tel: +90 262 6773110; Fax: +902626772309; Email: fevzihan.basarir@tubitak.gov.tr**Received:** November 06, 2014; **Accepted:** December 03, 2014; **Published:** December 04, 2014

Introduction

Increased demand for low-cost renewable energy sources has led to find alternative techniques to convert solar energy into electricity. Currently, conventional silicon based photovoltaic devices has dominated the market, however, their high cost is still a critical issue that limits their wide utilization [1]. Among all the alternative technologies, Bulk-Heterojunction (BHJ) type organic photovoltaic (OPV) seems the most promising one and is expected to play a major role in meeting the global renewable energy challenge in the near future. There are three key advantages of BHJ type OPVs; 1) polymer materials are inherently inexpensive, 2) they are compatible with plastic substrates and 3) they can be fabricated on large area using high-throughput and low temperature approaches [2].

Particularly, OPV devices containing blends of poly(3-hexylthiophene) (P3HT) and [6,6]-phenyl-C61-butyric acid methyl ester (PCBM) in the active layer have been widely studied and power conversion efficiency(PCE) of~3-5% have been reported by various research groups [3-7]. One of the key issues of achieving higher PCE is sufficient photon absorption in the active layer. However, increasing the thickness of active layer inevitably results in increased device resistance, owing to the low carrier mobility of organic materials. Thus, in order to improve the absorbance of active layer, various light trapping techniques have been tried such as periodic diffractive structures [8], V-shaped configurations [9], optical spacer layers [10], photonic crystals [11], and plasmonic metallic Nanoparticles (NPs) [12-15].

Enhanced light harvesting via utilization of metal NPs due to surface plasmon resonance characteristic is the most promising and efficient route among the mentioned approaches [16]. The

Abstract

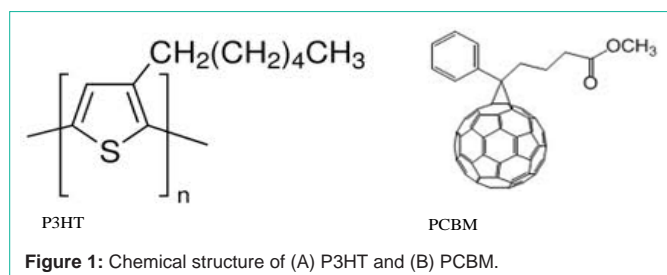
Bio-synthesized gold nanoparticles (AuNPs) with bacteria have been used to enhance the efficiency of P3HT: PCBM based Organic Photovoltaic (OPV) devices. First, AuNPs were synthesized in *Bacillus Subtilis* containing medium and characterized by zeta potential analyzer, energy dispersive X-ray spectrometer (EDS), UV-Vis spectrometer and Transmission Electron Microscope (TEM). The shape of AuNPs was found to be mainly spherical with an average diameter of 8.01 nm bearing negative surface charge (pH: 2~11). Next, the AuNPs were added to the PEDOT: PSS solution and spin-coated on the ITO substrate, followed by coating the active layer (P3HT:PCBM) and deposition of the metal electrodes. It has been observed that the power conversion efficiency (PCE) increased from 2.98 to 3.39% (enhancement of 14%) at optimum conditions by incorporation of bio-synthesized AuNPs in the whole transport layer.

Keywords: Organic photovoltaic; Gold nanoparticles; Bio-synthesis; P3HT: PCBM; Efficiency enhancement

excitation of surface Plasmon occurs through the interaction between the electromagnetic field of incident light and the surface electron density surrounding NPs, which led to local enhancement in the electromagnetic field. Moreover, metallic NPs can scatter and reflect the incident light, resulting in increased length of the optical path within the BHJ active layer film. Thus, the excitation of surface plasmon is very beneficial for improving light absorption and thus the photocurrent in OPVs [17].

Typically, plasmonic metal NPs are prepared through physical and chemical techniques. Physical techniques include the formation of AuNPs and AgNPs via thermal evaporation [18], electron beam evaporation [19], physical vapor deposition [20], laser-assisted nanofabrication [21], pulsed laser and ion beam milling [22]. Significant improvements has been achieved in PCE of the OPV devices via incorporation of the NPs, owing to light absorption enhancement and light scattering, which led to more light harvesting. However, these methods have various drawbacks such as high capital cost of the equipments, complex process, low throughput, poor control over size and shape of the nanoparticles and difficulty to work on large areas. In addition, the metal NPs could be only formed on ITO substrate, owing to the possible damage on the organic layers.

Consequently, the chemically synthesized AuNPs and AgNPs have been widely utilized for efficiency enhancement in OPV devices. Similar to physically obtained NPs, chemically synthesized counterparts also contribute to the PCE enhancement prominently in OPV devices [23-26]. Since they are prepared in colloidal forms, the metal NPs could be easily mixed with polymer solution, thus, they could be incorporated in whole transport and/or active layer. In addition, it is easy to control size/shape of the NPs and large quantities could be obtained in a short time. However, the chemical



synthesis methods usually contain toxic chemicals and may require high temperature and generate chemical wastes.

Microorganisms, such as bacteria, yeast and fungi, are known to produce inorganic materials either intra- or extracellularly [27-31]. Consequently, during the last decade, the bio-synthesis of metal NPs has been explored as an alternative since it is environmentally clean process. New alternatives for the synthesis of metallic NPs are currently being explored via bacteria, yeast, fungi, plant biomass, live plants and plant extracts. The use of biological systems for the synthesis of NPs offers several advantages since the methods are easier to carry out and more economical than traditional ones [32-35].

Thus, in this work, bio-synthesized AuNPs were prepared and utilized for efficiency enhancement in P3HT:PCBM based OPV devices. To our best knowledge, this is the first report on utilization of bio-synthesized AuNPs in OPVs. The AuNPs were synthesized by microbial bioconversion containing gold salt, followed by characterization. Then, the NPs were added to PEDOT:PSS solution and spin-coated on ITO substrate. Next, the fabrication of OPV device was completed by coating the active layer and deposition of metal electrode. The effect of AuNP concentration on the performance of OPV device was investigated. The characterization of OPV device was carried out with Lot-Oriel solar simulator under AM 1.5G conditions and the device efficiency was calculated.

Experimental

Materials

All reagents were purchased from commercial sources and used without further purification. [6, 6]-phenyl-C₆₁ butyric acid methyl ester (PC₆₁BM, defined as PCBM in the text) was purchased from Sigma-Aldrich (USA) while PEDOT-PSS (500P) was obtained from Clevios (Germany). The blend for the active layer was prepared by dissolving 25 mg of P3HT and PCBM in 1, 2 dichlorobenzene (1 ml). The structure of P3HT and PCBM was shown in Figure 1. Gold(III) chloridetrihydrate (HAuCl₄·3H₂O), microbiological media and its ingredients were purchased from Sigma-Aldrich (USA) and used as received.

Synthesis and characterization of AuNPs

Preparation of cell-free extracts: *Bacillus subtilis* strain, SDP1, isolated from the rhizosphere of *Acacia cyanophylla* Lindley has been used for the synthesis of AuNPs. In our unpublished work, taxonomic characterization of the said strain was determined by using morphological, physiological and molecular methods such as 16S rRNA analysis. The sequence has been submitted to the genbank with the accession number of **HM235916**. The bacteria cells were grown in nutrient broth at 37°C under shaking with 200 rpm for 24 hours. The cells were harvested by centrifugation (8.500 rpm, 20

min) and the culture supernatant was filtered through 22 μm filter to remove cell debris. Finally, pH of the supernatant was set to pH 9.0 with sufficient amount of NaOH.

Synthesis of AuNPs by cell-free extracts: Synthesis of AuNPs was carried out in a Schott bottle with final volume of 50 mL, which included equal volume of 1 mM HAuCl₄ solution and cell-free supernatant solution. The control sample did not contain any cell-free extract. The medium was subjected to microwave irradiation (Arçelik MD 585) at the frequency of 2.45 GHz with power output of 340 Watt in 60 s on/off cyclic mode. The irradiation process was conducted for 17 cycles. After two or three cycles, it was observed that the color of the solution changed from light yellow to shining red, indicating the formation of AuNPs.

Characterization of AuNPs: The AuNPs were characterized by TEM (JEM-2100, JEOL, Japan) and average particle size as well as particle size distribution were calculated by measuring particles manually from the TEM images. Zeta potential of the nanoparticle solution was determined by the Zetasizer (Malvern, Nanosz 3600) while the UV/Vis absorbance of the AuNP solution was measured by UV/Vis spectrometer (Becman DU 800).

Film and device fabrication

Indium Tin Oxide (ITO) coated glasses with sheet resistances of 25 Ω/cm were used as substrates. First, the substrates were cleaned in an ultrasonic bath with acetone, isopropyl alcohol, and deionized-water subsequently for 5 min and then dried under nitrogen gas flow. The solar cells were fabricated in the configuration of the traditional sandwich structure with ITO/PEDOT: PSS/active layer/Ca/Al. The PEDOT: PSS solution was spin coated on ITO coated glass substrates, flowed by annealing at 100°C for 30 minutes. The AuNPs were added in PEDOT:PSS solution with 1, 3 and 4% of weight. No problem in mixing of PEDOT: PSS and AuNP solution was observed since both are soluble or dispersible in water. The P3HT and PCBM solutions were prepared with 1:1 ratio and then the blend solution was spin coated on PEDOT: PSS coated substrate and finally, the cathode was thermally evaporated with Ca/Al at a pressure of 6x10⁻⁶ mbar through a shadow mask.

Device characterization

The current density-voltage (J-V) characteristics of devices were taken under light illumination using standard solar irradiation of 100 mW/cm² (AM1.5) with Xenon lamp as a light source and computer-controlled voltage-current Keithley 2600 source meter at 25°C under ambient atmosphere.

The Incident Photon to Current Efficiency (IPCE) measurements was performed by using NewPort Quantum Efficiency Systems. The samples were illuminated with monochromatic light of a Xenon lamp. The % IPCE was calculated according to the following equation:

$$\text{IPCE (\%)} = \frac{I_x \times 1240}{P_{in} \times \lambda_{incident}}$$

where I_{sc} (μA/cm²), P_{in} (W/m²) and λ (nm) is the measured current under short-circuit condition, the incident light power and the incident photon wavelength, respectively.

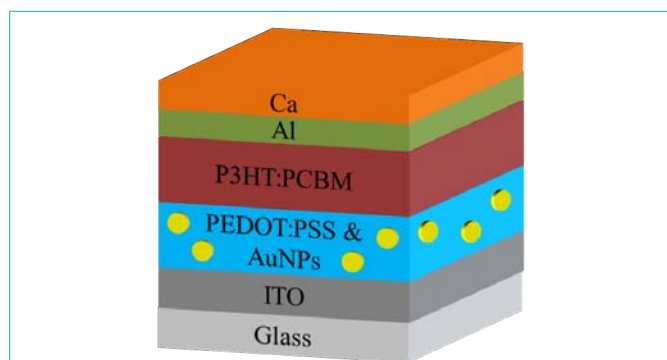


Figure 2: Device architecture of polymer solar cell.

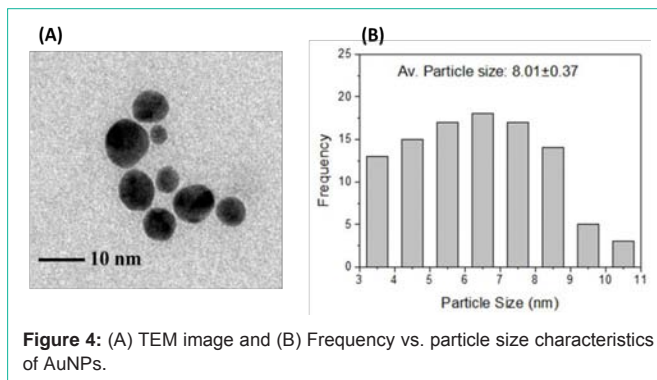


Figure 4: (A) TEM image and (B) Frequency vs. particle size characteristics of AuNPs.

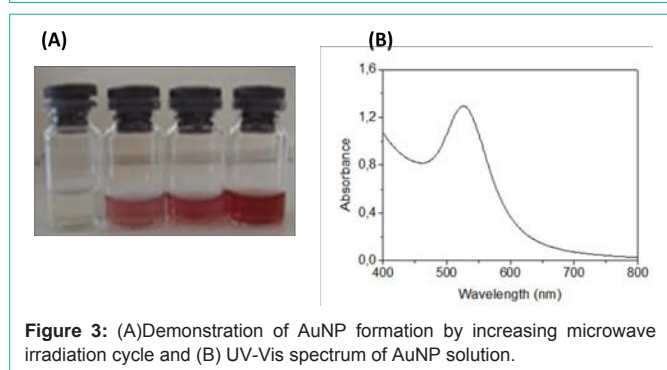


Figure 3: (A) Demonstration of AuNP formation by increasing microwave irradiation cycle and (B) UV-Vis spectrum of AuNP solution.

Results and Discussion

Synthesis and characterization of AuNPs

AuNPs were successfully synthesized using the microwave irradiation method. Nanoparticle formation was clearly observed by naked eye, following the change in color of the solution after microwave irradiation (Figure 3-A). Maximum absorption at about 530 nm (Figure 3-B) could be attributed to the surface plasmon resonance (SPR) of AuNPs, consistent with the previous reports [23,24]. Gradual increase in the intensity of the absorption band at 530 nm with increasing irradiation cycle was observed and maximum absorbance value was obtained at 17th cycle.

Transmission Electron Microscopy (TEM) micrograph (Figure 4-A) shows the size and shape of the nanoparticles. The size of the particles was calculated manually from the images and the average size was found as 8.01±0.37 nm (Figure 4-B). Well dispersed nanoparticles without any agglomeration in spherical shape were observed in the micrograph.

Zeta potential of the nanoparticles was measured as -33 mV thereafter the reaction. Effect of pH change on zeta potential was also determined as seen in Figure 5. In acidic pH range, until pH 4, zeta potential value does not change significantly and it was found as -15mV. However, as the pH was increased from 4 to 5, it drops abruptly until -27.5 mV. Thereafter, no sharp change was observed. It is also worthy to note that particles have more stable zeta potential values in basic pH range.

The actual mechanism for the biosynthesis of GNPs by different microorganisms is still not well understood. Some of the microorganisms growing at high metal ion concentrations are able to survive either by reducing or eliminating toxic effect of metals by

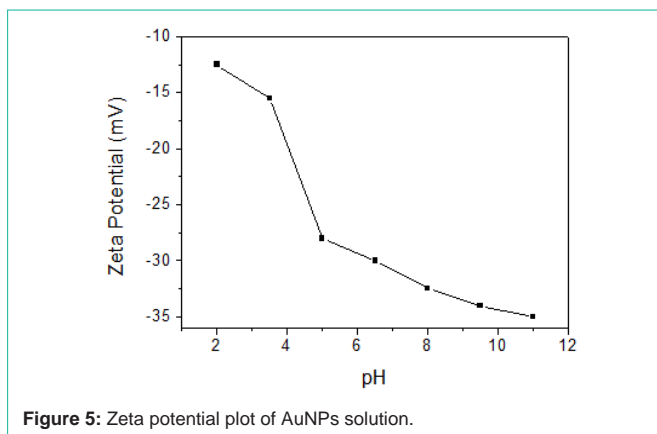


Figure 5: Zeta potential plot of AuNPs solution.

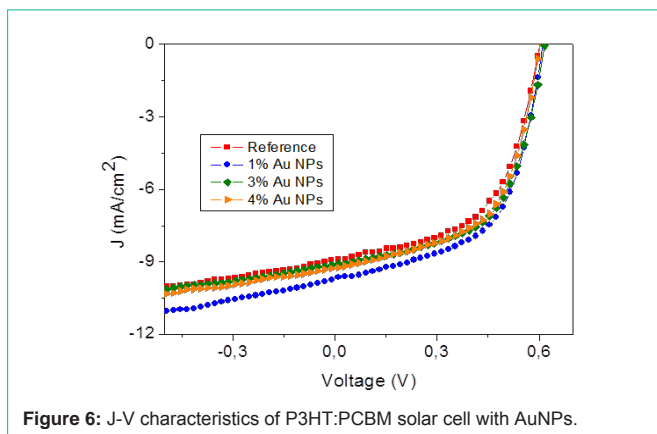


Figure 6: J-V characteristics of P3HT:PCBM solar cell with AuNPs.

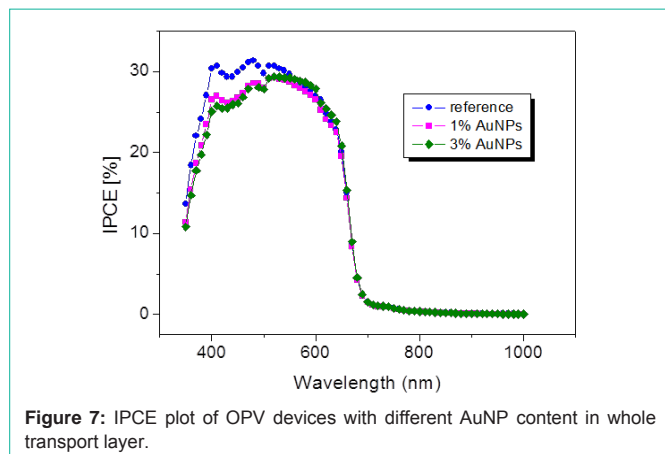
changing redox state of metal ions. Upon the change of redox state, metal nanoparticles form and precipitate intracellularly from the metal ion. However, it can be speculated that a specific reductase enzyme present in microorganism would be responsible for the reduction of metal ions to metallic nanoparticles [31]. On the other hand, metal ions trapped on the surface of the cells come together with reducing ions in the presence of enzymes, which led to formation of nanoparticles extracellularly [36].

Characterization of solar cell

Effect of AuNPs on device efficiency was investigated by embedding AuNPs in PEDOT: PSS layer. Figure 6 shows the current density–voltage measurements of the OPV devices with different AuNP concentration in the hole transport layer, which was recorded under 100 mW/cm² illumination (AM 1.5G). The reference device

Table 1: Summary of OPV device parameters.

Conc. of AuNP (%)	Voc	Jsc	FF	PCE
0	0.60	8.92	0.56	2.98
1	0.61	9.68	0.57	3.39
2	0.61	9.11	0.57	3.23
3	0.60	9.67	0.54	3.21

**Figure 7:** IPCE plot of OPV devices with different AuNP content in whole transport layer.

possessing the structure of ITO/PEDOT: PSS/P3HT: PCBM/Ca/Al has shown typical characteristics consistent with previous reports with an open-circuit voltage (V_{oc}) of 0.60 V, a short-circuit current (J_{sc}) of 8.92 mA/cm² and Fill Factor (FF) of 56%, resulting in a PCE of 2.98% [23,26]. In addition, it was found that current densities were improved with embedding plasmonic AuNPs compared to the reference device containing no AuNPs.

Detailed analysis of the OPV devices is demonstrated in Table 1. By adding 1% AuNP in whole transport layer, the PCE was substantially improved from 2.98 % to 3.39%. This could be mainly explained by the significant enhancement of short circuit current (J_{sc}) from 8.92 mA/cm² to 9.68 mA/cm². The Fill Factor (FF) was slightly improved and the open Circuit Voltage (V_{oc}) was mostly unchanged, suggesting that the PCE enhancement resulted fundamentally from the plasmonic effect of incorporated AuNPs [23,24,37].

IPCE values of P3HT: PCBM based POV devices with different AuNP concentration were shown in Figure 7, which indicated that photocurrent generation has been improved with addition of AuNP compared to reference cell. The best result for photocurrent generation was obtained with 1% AuNP concentration since photocurrent generation is increased from 18% to 30% (Figure 7). However, increasing the concentration of AuNPs (higher than 1%) has led to decreased PCE, possibly owing to the spoiled morphology of hole transport layer [12].

Conclusion

In summary, we have demonstrated the efficiency enhancement of P3HT: PCBM based OPV device via incorporation of biologically synthesized AuNPs in the PEDOT:PSS layer. The AuNPs with average size of 8.01 nm were successfully synthesized by *Bacillus subtilis* strain. It was found that adding 1% AuNP in whole transport layer has increased the device PCE from 2.98 to 3.39%. The 13% increment in the device efficiency was attributed to the enhanced light absorption

by the surface plasmon of the AuNPs.

Acknowledgement

The authors would like to acknowledge the financial support from FP7 (Grant No: PEOPLE-2011-CIG-303779), TÜBİTAK (Grant No: 111M510) and Materials Institute of TÜBİTAK Marmara Research Center.

References

- Soga T. Chapter 1 - Fundamentals of Solar Cell. Tetsuo S, editor. In: Nanostructured Materials for Solar Energy Conversion. Amsterdam: Elsevier. 2006; 3-43.
- Dennler G, Scharber MC, Brabec CJ. Polymer-Fullerene Bulk-Heterojunction Solar Cells. *Advanced Materials*. 2009; 21:1323-1338.
- Kim SS, Na SI, Kang SJ, Kim DY. Annealing-free fabrication of P3HT:PCBM solar cells via simple brush painting. *Sol Energy Mat Sol C*. 2010; 94:171-175.
- Dang MT, Wanz G, Bejbouji H, Urien M, Dautel OJ, Vignau L, et al. Polymeric solar cells based on P3HT:PCBM: Role of the casting solvent. *Sol Energy Mat Sol C*. 2011; 95: 3408-3418.
- Hegde R, Henry N, Whittle B, Zang H, Hu B, Chen J, et al. The impact of controlled solvent exposure on the morphology, structure and function of bulk heterojunction solar cells. *Sol Energy Mat Sol C*. 2012; 107: 112-124.
- Song Y, Ryu SO. The Optical and Electrical Characterization of Solar Cell Devices Based on the Physical Parameters of P3HT:PCBM Photoactive Layers. *Molecular Crystals and Liquid Crystals*. 2012; 565: 22-31.
- Shin WS, Hwang YM, So WW, Yoon SC, Lee CJ, Moon SJ. Performance of P3HT/C70-PCBM Polymer Photovoltaic Devices According to Manufacturing Conditions. *Molecular Crystals and Liquid Crystals*. 2008; 491: 331-338.
- Cocoyer C, Rocha L, Sicot L, Geffroy B, de Bettignies R, Sentain C, et al. Implementation of submicrometric periodic surface structures toward improvement of organic-solar-cell performances. *Applied Physics Letters*. 2006; 88: 133108.
- Rim SB, Zhao S, Scully SR, McGehee MD, Peumans P. An effective light trapping configuration for thin-film solar cells. *Applied Physics Letters*. 2007; 91: 243501.
- Kim JY, Kim SH, Lee HH, Lee K, Ma W, Gong X, et al. New Architecture for High-Efficiency Polymer Photovoltaic Cells Using Solution-Based Titanium Oxide as an Optical Spacer. *Advanced Materials*. 2006; 18: 572-576.
- Ko DH, Tumbleston JR, Zhang L, Williams S, DeSimone JM, Lopez R, Samulski ET. Photonic crystal geometry for organic solar cells. *Nano Lett*. 2009; 9: 2742-2746.
- Parlak EA, Asli Tumay T, Tore N, Sarioglan S, Kavak P, Türksoy F. Efficiency improvement of PCDTBT solar cells with silver nanoparticles. *Sol Energy Mat Sol C*. 2013; 110: 58-62.
- Kim K, Carroll DL. Roles of Au and Ag nanoparticles in efficiency enhancement of poly (3-octylthiophene)/C[60] bulk heterojunction photovoltaic devices. *Applied Physics Letters*. 2005; 87: 203113.
- Tore N, Parlak E, Tumay T, Kavak P, Sarioglan S, Bozar S, et al. Improvement in photovoltaic performance of anthracene-containing PPE-PPV polymer-based bulk heterojunction solar cells with silver nanoparticles. *J Nanopart Res*. 2014; 16: 1-8.
- Luan X, Wang Y. Plasmon-enhanced Performance of Dye-sensitized Solar Cells Based on Electrodeposited Ag Nanoparticles. *Journal of Materials Science & Technology*. 2014; 30: 1-7.
- Stratakis E, Kymakis E. Nanoparticle-based plasmonic organic photovoltaic devices. *Materials Today*. 2013; 16: 133-146.
- Gan Q, Bartoli FJ, Kafafi ZH. Plasmonic-enhanced organic photovoltaics: breaking the 10% efficiency barrier. *Adv Mater*. 2013; 25: 2385-2396.
- Westphalen M, Kreibig U, Rostalski J, Lüth H, Meissner D. Metal cluster enhanced organic solar cells. *Sol Energy Mat Sol C*. 2000; 61: 97-105.

19. Hou Y, Li S, Ye S, Shi S, Zhang M, Shi R, et al. Using self-assembly technology to fabricate silver particle array for organic photovoltaic devices. *Microelectronic Engineering*. 2012; 98: 428-432.
20. Kumar V, Wang H. Plasmonic Au nanoparticles for enhanced broadband light absorption in inverted organic photovoltaic devices by plasma assisted physical vapour deposition. *Organic Electronics*. 2013; 14: 560-568.
21. Beliatas MJ, Henley SJ, Han S, Gandhi K, Adikaari AADT, Stratakis E, et al. Organic solar cells with plasmonic layers formed by laser nanofabrication. *Physical Chemistry Chemical Physics*. 2013; 15: 8237-8244.
22. Lindquist NC, Luhman WA, Oh SH, Holmes RJ. Plasmonic nanocavity arrays for enhanced efficiency in organic photovoltaic cells. *Applied Physics Letters*. 2008; 93: 123308.
23. Hsiao YS, Charan S, Wu FY, Chien FC, Chu CW, Chen P, et al. Improving the Light Trapping Efficiency of Plasmonic Polymer Solar Cells through Photon Management. *The Journal of Physical Chemistry C*. 2012; 116: 20731-2037.
24. Chen FC, Wu JL, Lee CL, Hong Y, Kuo CH, Huang MH. Plasmonic-enhanced polymer photovoltaic devices incorporating solution-processable metal nanoparticles. *Applied Physics Letters*. 2009; 95: 013305.
25. Lee JH, Park JH, Kim JS, Lee DY, Cho K. High efficiency polymer solar cells with wet deposited plasmonic gold nanodots. *Organic Electronics*. 2009; 10: 416-420.
26. Wu JL, Chen FC, Hsiao YS, Chien FC, Chen P, Kuo CH, et al. Surface plasmonic effects of metallic nanoparticles on the performance of polymer bulk heterojunction solar cells. *ACS Nano*. 2011; 5: 959-967.
27. Ahmad A, Senapati S, Khan MI, Kumar R, Ramani R, Srinivas V, et al. Intracellular synthesis of gold nanoparticles by a novel alkalotolerant actinomycete, *Rhodococcus* species. *Nanotechnology*. 2003; 14: 824-828.
28. Senapati S, Ahmad A, Khan MI, Sastry M, Kumar R. Extracellular biosynthesis of bimetallic Au-Ag alloy nanoparticles. *Small*. 2005; 1: 517-520.
29. Mukherjee P, Roy M, Mandal BP, Dey GK, Mukherjee PK, Ghatak J, et al. Green synthesis of highly stabilized nanocrystalline silver particles by a non-pathogenic and agriculturally important fungus *T. asperellum*. *Nanotechnology*. 2008; 19: 075103.
30. Pum D, Sleytr UB. The application of bacterial S-layers in molecular nanotechnology. *Trends in Biotechnology*. 1999; 17: 8-12.
31. Nangia Y, Wangoo N, Goyal N, Shekhawat G, Suri C. A novel bacterial isolate *Stenotrophomonas maltophilia* as living factory for synthesis of gold nanoparticles. *Microbial Cell Factories*. 2009; 8: 39.
32. Golmoraj VE, Reza Khoshayand M, Amini M, Mollazadeh Moghadam K, Amin G, Reza Shahverdi A. The surface chemistry and stability of gold nanoparticles prepared using methanol extract of *Eucalyptus camaldulensis*. *Journal of Experimental Nanoscience*. 2011; 6: 200-208.
33. Bar H, Bhui DK, Sahoo GP, Sarkar P, Pyne S, Chattopadhyay D, et al. Synthesis of gold nanoparticles of variable morphologies using aqueous leaf extracts of *Cocculus hirsutus*. *Journal of Experimental Nanoscience*. 2011; 7: 109-19.
34. Kesarla MK, Mandal BK, Bandapalli PR. Gold nanoparticles by *Terminalia bellirica* aqueous extract – a rapid green method. *Journal of Experimental Nanoscience*. 2012; 9: 825-830.
35. Dhanasekaran D, Latha S, Saha S, Thajuddin N, Panneerselvam A. Extracellular biosynthesis, characterisation and *in-vitro* antibacterial potential of silver nanoparticles using *Agaricus bisporus*. *Journal of Experimental Nanoscience*. 2012; 8: 579-588.
36. Zhang X, Yan S, Tyagi RD, Surampalli RY. Synthesis of nanoparticles by microorganisms and their application in enhancing microbiological reaction rates. *Chemosphere*. 2011; 82: 489-494.
37. Baek SW, Noh J, Lee CH, Kim B, Seo MK, Lee JY. Plasmonic Forward Scattering Effect in Organic Solar Cells: A Powerful Optical Engineering Method. *Sci Rep*. 2013; 3.